Monthly Notices of the ROYAL ASTRONOMICAL SOCIETY

Mon. Not. R. Astron. Soc. **400,** 1472–1478 (2009) doi:10.1111/j.1365-2966.2009.15546.x

A Keck/DEIMOS spectroscopic survey of the faint M 31 satellites And XV and And XVI

B. Letarte,[1] S. C. Chapman,[2★] M. Collins,[2] R. A. Ibata,[3] M. J. Irwin,[2] A. M. N. Ferguson,[4] G. F. Lewis,[5] N. Martin,[6] A. McConnachie[7] and N. Tanvir[8]

[1]*California Institute of Technology, 1200 E. California Blvd, MC 105-24, Pasadena, CA 91125, USA*
[2]*Institute of Astronomy, Madingley Road, Cambridge CB3 0HA*
[3]*Observatoire de Strasbourg, 11, rue de l'Université, F-67000 Strasbourg, France*
[4]*Institute for Astronomy, University of Edinburgh, Royal Observatory, Blackford Hil l, Edinburgh EH9 3HJ*
[5]*Institute of Astronomy, School of Physics, A29, University of Sydney, NSW 2006, Australia*
[6]*Max-Planck-Institut fur Astronomie, Konigstuhl 17, D-69117 Heidelberg, Germany*
[7]*Department of Physics and Astronomy, University of Victoria, Victoria, B.C. V8P 1A1, Canada*
[8]*Department of Physics and Astronomy, University of Leicester, Leicester LE17RH*

Accepted 2009 August 14. Received 2009 August 12; in original form 2009 January 7

ABSTRACT

We present the results of a spectroscopic survey of the recently discovered M31 satellites And XV and And XVI, lying at projected distances from the centre of M31 of 93 and 130 kpc, respectively. These satellites lie to the south of M31, in regions of the stellar halo which wide-field imaging has revealed as relative *voids* (compared to the ∼degree-scale coherent stream-like structures). Using the Deep Imaging Multi-Object Spectrograph mounted on the Keck II telescope, we have defined probable members of these satellites, for which we derive radial velocities as precise as ∼6 km s^{-1} down to $i \sim 21.5$. While the distance to And XVI remains the same as previously reported (525 ± 50 kpc), we have demonstrated that the brightest three stars previously used to define the tip of the red giant branch in And XV are in fact Galactic, and And XV is actually likely to be much more distant at 770 ± 70 kpc (compared to the previous 630 kpc), increasing the luminosity from $M_{\rm V} \approx -9.4$ to -9.8. The And XV velocity dispersion is resolved with $v_r = -339^{+7}_{-6}$ km s^{-1} and $\sigma_v = 11^{+7}_{-5}$ km s^{-1}. The And XVI dispersion is not quite resolved at 1σ with $v_r = -385^{+5}_{-6}$ km s^{-1} and $\sigma = 0^{+10}_{-\rm indef}$ km s^{-1}. Using the photometry of the confirmed member stars, we find metallicities of And XV (median [Fe/H] = −1.58, interquartile range ±0.08) and And XVI (median [Fe/H] = −2.23, interquartile range ±0.12). Stacking the spectra of the member stars, we find spectroscopic [Fe/H] = −1.8 (−2.1) for And XV (And XVI), with an uncertainty of ∼0.2 dex in both cases. Our measurements of And XV reasonably resolve its mass (∼10^8 M$_\odot$) and suggest a polar orbit, while the velocity of And XVI suggests it is approaching the M31 escape velocity given its large M31 centric distance.

Key words: galaxies: dwarf – galaxies: individual: And XV – galaxies: individual: And XVI – Local Group – galaxies: stellar content.

1 INTRODUCTION

In recent years, systematic searches have been performed in earnest within the Local Group, both photometrically and spectroscopically, in order to fully catalogue its population of satellite galaxies. There are several motivations behind these endeavours, with one of the more hotly discussed being that of the so-called 'missing satellites problem' (Moore et al. 1999; Klypin et al. 1999), which is an observed discrepancy of one to two orders of magnitude between the number of satellite galaxies produced within cosmological simulations and the number we see orbiting the Galaxy and M31 today. Whilst these surveys have approximately doubled the known satellite populations of both galaxies within recent years (Zucker et al. 2004; Willman et al. 2005; Chapman et al. 2005; Belokurov et al. 2006; Martin et al. 2006; Zucker et al. 2006a, 2006b; Belokurov et al. 2007; Majewski et al. 2007; Irwin et al. 2008), we are still far from reconciling the observations with simulations. Several theories have been put forward in order to address this issue. Survey completeness is a widely debated topic (see e.g. Simon & Geha 2007; Tollerud et al. 2008), particularly with respect to the Milky Way (MW), where observational efforts are hampered by

★E-mail: schapman@ast.cam.ac.uk

obscuration from the disc and the bulge. Future all-sky surveys may find a wealth of ultrafaint satellites that would alleviate this gap between observation and theory. Another proposed solution is that the satellite galaxies within the Local Group inhabit increasingly dark-matter-dominated haloes as they become fainter (Bullock, Kravstov & Weinberg 2000; Stoehr et al. 2002), so that even the faintest of dwarf galaxies would reside within massive dark matter haloes.

Peñarrubia, McConnachie & Babul (2006), Peñarrubia, McConnachie & Navarro (2008a) and Peñarrubia, Navarro & McConnachie (2008b) demonstrate that within the Λ cold dark matter working frame dwarf spheroidal galaxies (dSphs) are well embedded within the dark matter haloes that surround them. For the brightest dwarf galaxies in the MW, they find that $0.01 < R_c/r_s < 0.1$, where R_c and r_s are the stellar core radius and the NFW scaleradius, respectively. That implies that these systems are fairly resilient to tidal interactions, so that they can lose a large fraction of their initial dark matter mass before the stellar component starts being disrupted.

An observational test of these suggestions is then to measure the stellar light and dynamical mass of faint dwarf galaxies in the Local Group. With spectroscopic information, one can measure the central velocity dispersion of the satellite, which has been shown to be a good indicator of the instantaneous mass of a dwarf galaxy within the radii of the luminous tracers (e.g. Oh, Lin & Aarseth 1995; Piatek & Pryor 1995), even if the dwarf is not in virial equilibrium or perfectly spherical. Several approaches have been taken to derive the total mass of the system from the central velocity dispersion (e.g. Illingworth 1976; Richstone & Tremaine 1986; Gilmore et al. 2007). Recent detailed modelling of dwarf galaxy velocity dispersions suggests a lower dynamical mass limit of $\sim 10^7$ $M_\odot$ (Strigari et al. 2008).

Spectroscopic data on the dSphs of the Local Group is also desirable in order to give us a better understanding of the nature of these tiny galaxies. The discovery and study of the faintest members of this population has shown that at the low-luminosity end of the spectrum these satellites do not behave as expected from the study of their brighter counterparts. In particular, they begin to deviate significantly from established trends between mass and metallicity, and mass-to-light ratio versus light. In the brighter MW dwarfs, the lack of very metal poor stars (Helmi et al. 2006), the stellar populations (Unavane, Wyse & Gilmore 1996) and differing abundance patterns from the MW halo (Shetrone, Cote & Sargent 2001) reinforce the point that the surviving, isolated dwarfs have different environmental conditions than those which phase mixed into the MW stellar halo. However, the ultrafaint MW satellites do show evidence of very metal poor stars (Kirby et al. 2008), possibly suggesting these dwarfs are remnants of the halo building blocks.

By acquiring kinematic data for the Local Group satellites, we can isolate the likely dwarf member stars from the colour–magnitude diagrams (CMDs), perform independent checks on the metallicities derived photometrically, and also estimate their total masses so we can place them more fully in the context of the dSph population, and determine if there truly is a breakdown in these relations at low luminosities, and if so at what point this divergence begins to take effect.

Another motivation behind obtaining kinematic data for the satellite populations of the MW and M31 is to achieve a greater understanding of the dynamics of the Local Group as a whole. The mass contained within the inner few 10's kpc of both is relatively well constrained from optical and HI data, as well as globular cluster and planetary nebulae tracer populations (see e.g. Kochanek 1996; Carignan et al. 2006), but probing the outer halo at large radii proves to be more of a challenge. An ideal method for measuring the *total* masses of the MW and M31 is to use their satellite galaxies as direct tracers of their potentials. As they are located at large distances from their hosts (∼few 100 kpc), they probe the full extent of their mass distributions. Such a method has been used previously in both the MW and M31 (Wilkinson & Evans 1999; Evans et al. 2000; Gottesman, Hunter & Boonyasait 2002); however, the associated errors on their measurements are huge (of the order of approximately twice the measurements themselves) due to the low number of satellite galaxies with reliable kinematic and distance data available to them. In the years since these results were published, more than 20 satellite companions of the MW and M31 have been discovered, many of which have also been studied spectroscopically. If kinematic data on all the satellites within the Local Group can be obtained, we will be able to better constrain the masses of these two 'sister' galaxies.

With these goals in mind, it remains crucial to obtain radial velocities for newly discovered dSphs in order to understand their mass distribution and orbital properties. As a step towards this end, we have used the Keck II Deep Imaging Multi-Object Spectrograph (DEIMOS) to derive radial velocities and metallicities of stars within two new satellites discovered in Ibata et al. (2007), And XV and And XVI.

2 OBSERVATIONS

Multi-object Keck observations with DEIMOS (Faber et al. 2003) for And XV and And XVI were made on 2007 October 8 and 9, in variable conditions (with 0.6–1.0 arscec seeing and patchy cirrus). To obtain improved signal-to-noise ratio (S/N) in a reasonable exposure time for the faint ($i = 20.5$–22.5) red giant branch (RGB) stars targeted, we employed the lower resolution 600 line mm^{-1} grating. For the Ca II triplet (CaT) lines, which are reasonably resolved at this lower ($R \sim 3000$) resolution, the trade-off is a strong function of the location of the spectral features of interest relative to the strong night sky OH recombination lines. While we detect continuum at S/N > 3 per Å over the CaT regions for faint ($i \sim 22$) stars, the velocity errors can suffer larger systematic errors when they lie close to OH lines, and the velocity accuracy can vary considerably with continuum S/N. Our chosen instrumental setting covered the observed wavelength range from 0.56 to 0.98 μm. Exposure time was 60 min on each dSph, split into 20-min integrations. Data reduction followed standard techniques using the DEIMOS–Deep Extragalactic Evolutionary Probe 2 (DEEP2) pipeline (Faber et al. 2003), debiasing, flat-fielding, extracting, wavelength-calibrating and sky-subtracting the spectra.

The radial velocities of the stars were then measured by fitting the peak of the cross-correlation function derived using a template spectrum consisting of delta functions to the instrumental resolution (3 Å) at the wavelengths of the CaT absorption lines. This procedure also provides an estimate of the radial velocity accuracy obtained for each measurement. The velocity uncertainties typically range from 6 to 25 km s^{-1}. Target stars were assigned from a broad (1 mag) box around the general outline of the RGB of the dwarf. A narrower box of 0.3 mag around the RGB was then constructed with higher priorities. In both of these selection boxes, the priority was scaled as a function of *i*-mag so that brighter stars had more chances of being observed. The remainder of the mask space was filled with target stars from a broad region encompassing RGB stars in M31 over all possible metallicities and distances. The And XV and And XVI masks had 143 and 131 target stars, respectively. The small number of candidate members compared to the total amount

of stars observed is simply due to the fact that the footprint of DEIMOS is much wider than the small angular size of the dwarf galaxies, therefore there are many more stars that are not part of the main dSph targets.

3 RESULTS

The spatial distributions of the stars in the regions of And XV and And XVI are shown in Fig. 1. Candidate member stars from the DEIMOS spectroscopy are highlighted (listed in Tables 1 and 2).

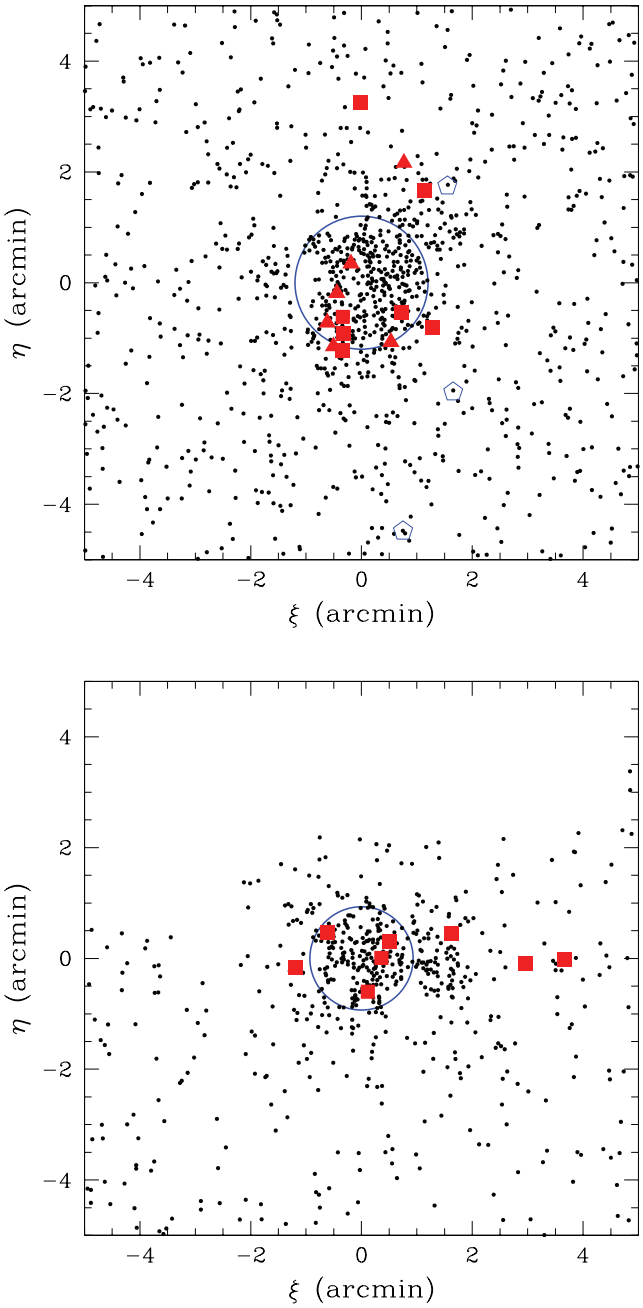

Figure 1. Spatial distribution of stars in the regions of And XV (top panel) and And XVI (bottom panel). Candidate member stars identified spectroscopically are highlighted as robust (filled squares) likely (filled triangles), and in the case of And XV three Galactic foreground stars which were previously identified as the tip of the RGB (pentagons). Circular half-light radii are overlaid.

Member stars are selected by having a velocity which lies within 2σ of the median of the obvious kinematic clumps of stars in each dwarf field. Note that for And XV the member stars are highlighted differently for *robust* and *tentative* members, defined below in terms of the strength of the cross-correlation peak in the velocity determination. Canada–France–Hawaii Telescope–MegaCam CMDs of stars within a 3-arcmin radius of And XV and And XVI are shown in Fig. 2, again with likely member stars highlighted. The red giant branches of both dwarfs are clearly visible, while the horizontal branches are reasonably detected. In the case of And XV, three stars previously assumed to lie near the tip of the red giant branch (TRGB) have been shown by their velocities and Na I doublet equivalent width (EW) to be foreground Galactic dwarf stars. We then revise the distance estimate of And XV from the 630 ± 60 kpc previously reported (Ibata et al. 2007), estimating the true tip of the RGB is ∼0.5 mag fainter than the $i = 20.4$ previously assumed. Adopting metallicity-corrected tip of the red giant branch = −4.04 ± 0.12 from Bellazzini, Ferraro & Pancino (2001) for the absolute I-band magnitude of the RGB tip, and convert into the Landolt system using the colour equations in Ibata et al. (2007) and those given by McConnachie et al. (2004); this yields a distance modulus of $m - M = 24.4 \pm 0.2$ or a distance of 770 ± 70 kpc (versus the previous 630 ± 60 kpc). This revised distance agrees with that obtained by considering the magnitude, $g \sim 25.3$, of the horizontal branch (Fig. 2). The change in distance increases the luminosity from $M_V \approx -9.4$ to −9.8. In And XVI, as all stars near the TRGB were confirmed spectroscopically as members of the dwarf spheroidal galaxy, the Ibata et al. (2007) distance estimate of 525 ± 50 kpc remains unchanged. The horizontal branch for And XVI (Fig. 2) at $g \sim 24.5$ (0.8 mag difference from And XVI) agrees well with our proposed 0.5-mag difference in the TRGB between the two dwarf spheroidals. In Fig. 2, we also overlay 13-Gyr old Padova isochrones with solar-scaled chemical compositions (Girardi et al. 2004), at the TRGB distance and median metallicity obtained from member stars (see below), providing a reasonable fit in both cases. The use of an old (13 Gyr) isochrone can be justified by the predominantly old nature of the majority of the recently detected M31 satellites.

The distribution of stars in And XV and And XVI is shown in Fig. 3 as a function of their radial velocity. The stars are then shown as a function of radius from the centres of the dwarfs with half-light radii indicated. Photometric [Fe/H] is estimated by comparison to Padova isochrones (Girardi et al. 2004) corrected for extinction (Schlegel, Finkbeiner & Davis 1998) and shifted to the revised distances of the dSphs. These [Fe/H] values are shown in Fig. 3 as a function of their radial velocity, revealing the tight range in metallicities of both And XV (median [Fe/H] = −1.58, interquartile range ± 0.08) and And XVI (median [Fe/H] = −2.23, interquartile range ±0.12). For And XV, the median [Fe/H] and its dispersion are identical using either the robust spectra or including the tentative spectra as well, lending further evidence to these stars likely being And XV members.

One-dimensional spectra of member stars in And XV and And XVI are shown in Figs 4 and 5, respectively. And XV spectra are separated into robust members with cross-correlation peak >0.2, and more tentative member stars with cross-correlation peak <0.2, but still lying on the well-defined RGB of And XV. The inverse variance weighted, summed spectrum is shown in the bottom offset panel for each dSph. All candidate member spectra for And XVI are considered to be robust by the above criteria. While not shown in the spectra, the Na I doublet is undetected significantly in the individual stars, and also in the stacked spectra. The Na I EW

Table 1. Properties of candidate member stars in And XV centred at $\alpha = 01^{h}14^{m}18.7^{s}, \delta = 38°07'03''$.

α (J2000)	δ (J2000)	v_r (km s^{-1})	[Fe/H]$_{spec}$	S/N$_{ctm}$ [b]	[Fe/H]$_{phot}$	g-mag	i-mag
01:14:16.28	38:05:49.6	-360.0 ± 6.3	-2.4	6.2	-1.45	22.75	21.26
01:14:16.34	38:06:08.2	-336.6 ± 5.6	-2.0	8.8	-1.47	22.50	20.86
01:14:24.52	38:06:14.6	-324.2 ± 18.3	-0.2	1.6	-1.59	23.81	22.78
01:14:16.30	38:06:25.9	-323.5 ± 14.7	-2.5	6.3	-1.61	22.59	21.19
01:14:21.64	38:06:31.0	-278.5 ± 52.4	-0.0	1.9	-1.93	23.54	22.56
01:14:23.84	38:08:43.3	-335.0 ± 23.4	-0.5	2.9	-1.58	23.44	22.32
01:14:17.94	38:10:18.2	-334.6 ± 6.1	-2.5	6.7	-1.58	22.64	21.24
01:14:21.90	38:09:13.0	-296.6 ± 12.5	-0.0	1.0	-1.30	24.95	23.97
01:14:15.43	38:05:54.2	-373.6 ± 21.0	-1.2	1.8	-1.61	23.07	21.97
01:14:20.70	38:05:58.9	-341.8 ± 25.3	-1.5	3.8	-1.46	23.19	21.93
01:14:14.86	38:06:19.8	-302.2 ± 22.5	-1.6	3.0	-1.73	22.90	21.81
01:14:15.74	38:06:51.8	-296.1 ± 22.2	-1.5	2.7	-1.85	22.80	21.71
01:14:17.04	38:07:23.8	-374.1 ± 16.3	-1.4	2.5	-1.44	23.27	22.06

[a]Candidate member stars in And XV are divided into a robust group (top seven) and a more tentative group (bottom six).
[b]S/N in the continuum, estimated over the 250 Å region surrounding the CaT.

Table 2. Properties of candidate member stars in And XVI centred at $\alpha = 0^{h}59^{m}30.0^{s}, \delta = 32°22'30''$.

α (J2000)	δ (J2000)	v_r (km s^{-1})	[Fe/H]$_{spec}$	S/N$_{ctm}$	[Fe/H]$_{phot}$	g-mag	i-mag
00:59:29.54	32:21:59.9	-373.5 ± 23.1	-2.7	3.3	-2.24	22.38	21.25
00:59:23.33	32:22:26.4	-369.4 ± 11.9	-2.2	6.2	-2.08	22.07	20.78
00:59:43.04	32:22:30.0	-380.1 ± 17.8	-1.2	1.1	-2.48	23.84	22.99
00:59:46.39	32:22:34.5	-389.0 ± 10.0	-1.6	9.1	-1.98	21.85	20.40
00:59:30.71	32:22:36.4	-409.8 ± 16.9	-2.3	6.8	-2.23	21.99	20.74
00:59:31.43	32:22:53.8	-400.5 ± 21.9	-0.9	6.8	-2.39	21.98	20.69
00:59:36.69	32:23:03.3	-391.3 ± 24.8	-1.8	2.6	-2.31	22.95	21.94
00:59:26.12	32:23:04.5	-381.4 ± 12.2	-2.4	6.0	-2.09	22.12	20.86

is sensitive to the surface gravity, and thus is a good discriminant of Galactic foreground dwarf stars (Schiavon et al. 1997), although at these large negative velocities the probability is very low that any identified star in our CMD selection box would be Galactic. Stars with velocities <150 km s^{-1}, consistent with Galactic stars typically have well-detected Na I doublet lines in our DEIMOS spectra. The spectroscopic [Fe/H] has very large errors in most of the individual spectra; however, a reasonable comparison can be made between the [Fe/H] derived from the stacked spectrum and the median photometric [Fe/H]. We find [Fe/H] $= -1.8$ (-2.1) for And XV (And XVI) by measuring the EW of the CaT lines as in Chapman et al. (2005), on the Carretta & Gratton (1997) scale. A large uncertainty, measured from the summed sky spectrum, of $\sim$0.2 dex is due primarily to sky-subtraction residuals making it difficult to define the continuum level of the spectrum. Koch et al. (2008) have also demonstrated that high-quality Keck/DEIMOS spectra of stars in the M31 halo are amenable to further chemical analysis, showing a range of species (mostly Fe I and Ti I lines) which become weaker for the more metal-poor stars. For And XV and And XVI, even the stacked spectra do not detect significant absorption at the Ti I lines (8378, 8426 and 8435 Å). Our stacked spectra do not have the requisite S/N to detect the anticipated EW based on stars of similar metallicity from Koch et al. (2008), although roughly tripling the S/N of the spectra would be more than sufficient ($\sim$4$\times$ integration time in typical Mauna Kea weather conditions, compared to the rather poor conditions under which the present data were taken).

For our samples of member stars with large and variable velocity errors (typically 6–25 km s^{-1}), the Maximum Likelihood approach (e.g. Martin et al.. 2007) provides a method to assess the true underlying velocity distribution of the dSphs. Fig. 6 shows the results of our analysis of And XV and And XVI plotting the one-dimensional distributions 1σ, 2σ, 3σ values. The And XV dispersion is resolved with $v_r = -339^{+7}_{-6}$ km s^{-1} and $\sigma_v = 11^{+7}_{-5}$ km s^{-1}, where little difference is found from using only the best seven member stars (from Fig. 4) versus using all 13 candidate members (including the six more tentative velocities measurements). The And XVI dispersion is not quite resolved at 1σ with $v_r = -385^{+5}_{-6}$ km s^{-1} and $\sigma = 0^{+10}_{-\mathrm{indef}}$ km s^{-1}.

4 DISCUSSION AND CONCLUSIONS

We have been able to further constrain the properties of the dSphs And XV and And XVI by measuring velocities and metallicities and assigning probable member stars to each galaxy. While this represents a significant addition to our knowledge about these dSphs compared to the photometric discovery and characterization (Ibata et al. 2007), our spectroscopic measurements are generally not precise enough to provide robust measures of the velocity dispersions. And XV has a most likely dispersion $\sim$10 km s^{-1} (while And XVI is more poorly constrained but has a 1σ upper limit of 10 km s^{-1}) which would translate to a $\sim 10^8$ M$_\odot$ halo mass using the method of Richstone & Tremaine (1986) as has been done for other M31 dSphs with better constrained velocity dispersions (e.g. Chapman et al. 2005; Majewski et al. 2007). This is similar to that proposed by Gilmore et al. (2007) for a limiting dark matter halo mass in the smallest galaxies; however, we cannot confidently rule out that the dispersions are smaller than our measurements suggest. Longer Keck/DEIMOS exposures under good conditions could

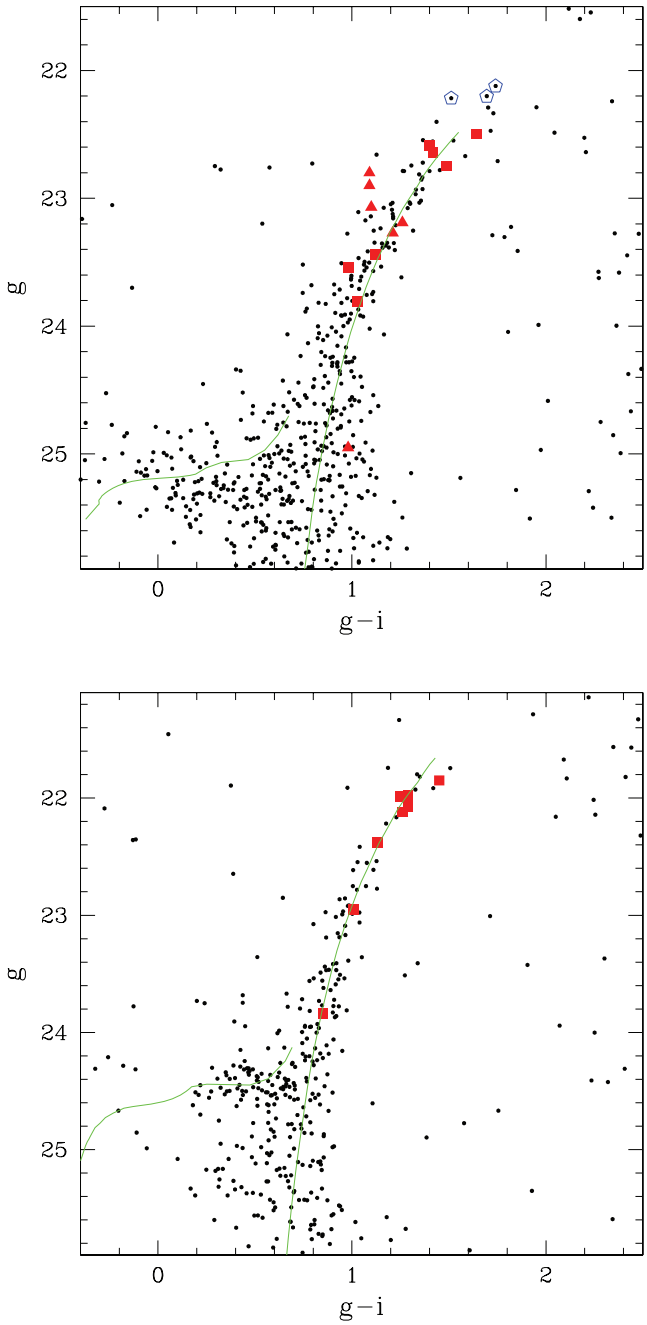

Figure 2. CFHT–MegaCam CMDs of stars within a 3 arcmin radius of And XV (top panel) and And XVI (bottom panel). The MegaCam mags are calibrated on Sloan Digital Sky Survey like system as AB magnitudes. The red giant branches of both dSphs are clearly visible, while the horizontal branch is reasonably detected in both the cases. Candidate member stars from the DEIMOS spectroscopy are highlighted (filled squares – robust members, filled triangles – tentative members). In the case of And XV, three stars previously assumed to lie near the TRGB have been shown by their velocities and Na I doublet EWs to be Galactic foreground (open pentagons). The revised TRGB and horizontal branch distance to And XV is 770 kpc as described in the text. 13-Gyr old Padova isochrones are overlaid, at the TRGB distance and median metallicity obtained from member stars, providing a reasonable fit in both the cases.

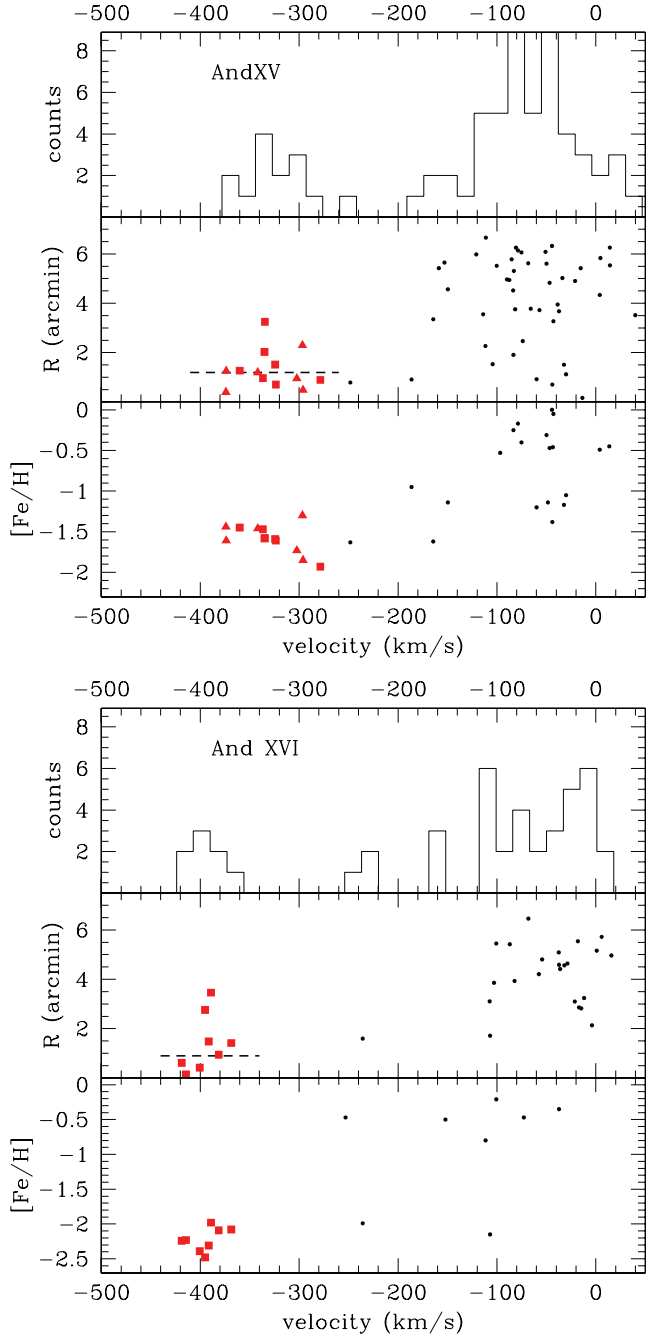

Figure 3. Distribution of stars in And XV (top), And XVI (bottom) as a function of their radial velocity (upper panels). The stars are then shown as a function of radius from the centres of the dSphs, with half-light radius drawn as a dashed line (middle panels). Photometric [Fe/H] as described in the text is shown in the bottom panels, revealing the tight range in metallicities of And XV ([Fe/H] ~ -1.6) and And XVI ([Fe/H] ~ -2.2). Symbols are highlighted as in Figs 1 and 2.

significantly improve these results. The relatively well-populated RGBs of both dSphs suggests that enough member stars could be obtained to begin to measure the velocity dispersion profile, a much more reliable constraint on the dark matter halo mass (Gilmore et al. 2007).

As mentioned, both dSphs lie in relative voids (free of degree-scale substructure) in the M31 halo maps of Ibata et al. (2007).

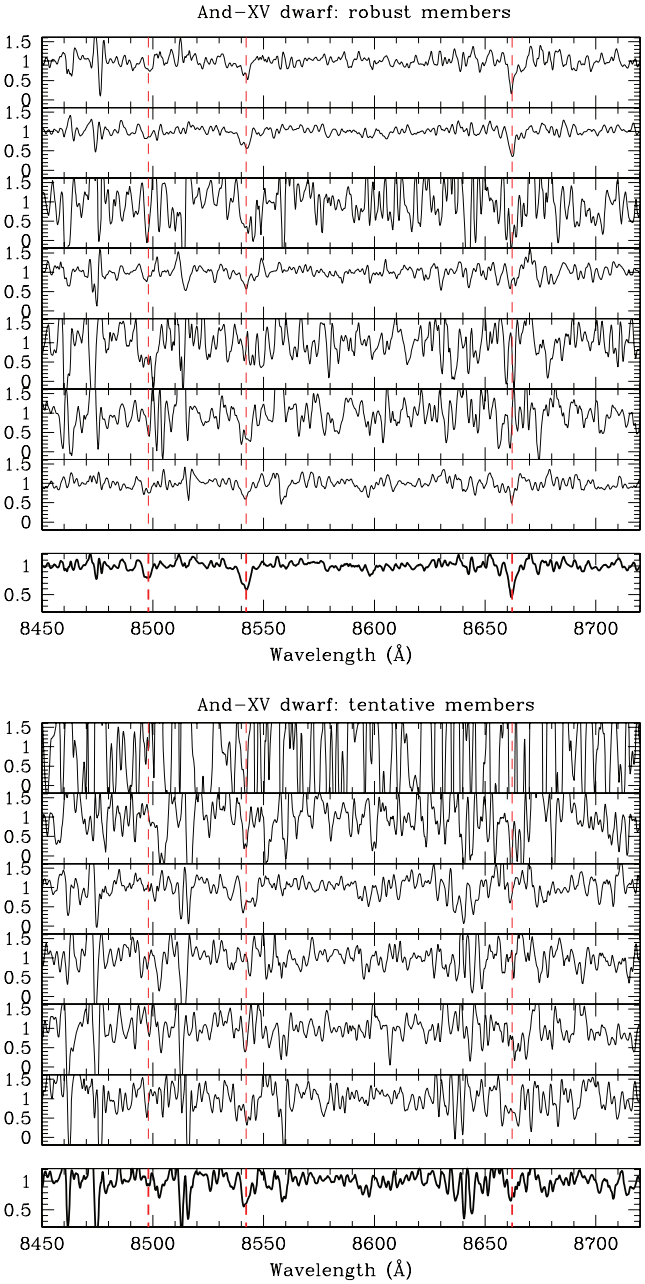

Figure 4. Spectra of candidate member stars in And XV. Top panel shows robust members with cross-correlation peak >0.2. Bottom panel shows more tentative member stars with cross-correlation peak <0.2, but still lying on the well-defined RGB of And XV. The inverse variance weighted summed spectrum is shown in the bottom offset panels for each subsample.

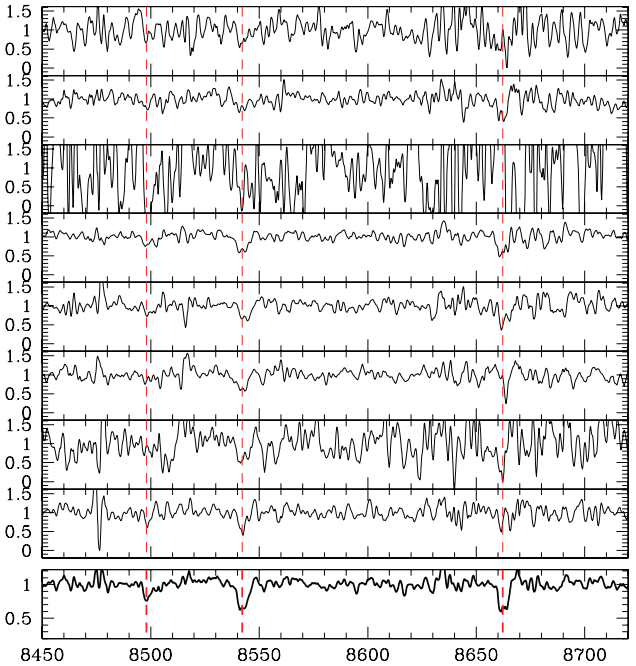

Figure 5. Spectra of candidate member stars in And XVI. The inverse variance weighted summed spectrum is shown in the bottom offset panel.

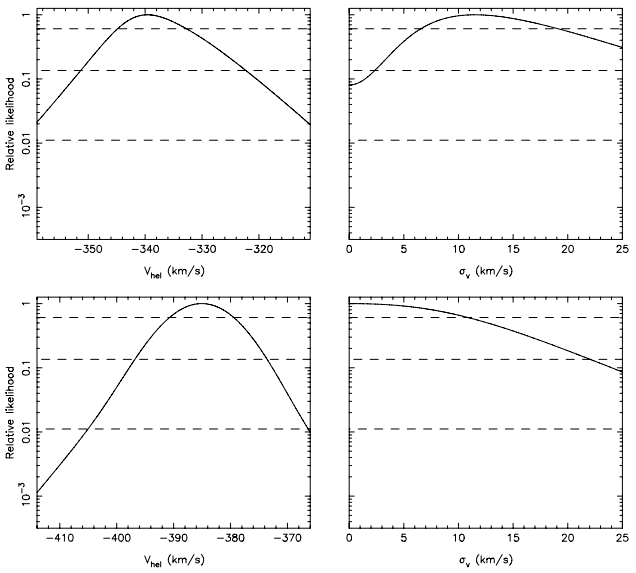

Figure 6. Likelihood distributions of member stars in And XV (top panels) and And XVI (bottom panels). The point shows the most likely values of radial velocity and velocity dispersion, dashed lines showing the 1σ, 2σ, 3σ distributions. For And XV, we show likelihood distributions of the seven best candidate members. The And XV dispersion is resolved with $v_r = -339^{+7}_{-6}\,\mathrm{km\,s^{-1}}$ and $\sigma_v = 11^{+7}_{-5}\,\mathrm{km\,s^{-1}}$. The And XVI dispersion is not quite resolved at 1σ with $v_r = -385^{+5}_{-6}\,\mathrm{km\,s^{-1}}$ and $\sigma = 0^{+10}_{-\mathrm{indef}}\,\mathrm{km\,s^{-1}}$.

In our spectroscopic samples, there are relatively few remaining M31 halo stars once the likely And XV and And XVI member stars and Galactic foreground are removed (three and six candidate halo stars, respectively, and some of these are likely to be Galactic by their proximity to the low-velocity regime of Milky Way stars). This is consistent with the extrapolated M31 halo profle (Ibata et al. 2007) out to 93 and 130 kpc, respectively. However, this suggests that significant spectroscopic efforts would be required to properly characterize the (substructure-free) halo in the 100–150 kpc regime. None the less, the average spectroscopic [Fe/H] = −1.5 of these nine confirmed M31 halo stars is consistent with a lack of metallicity gradient in the underlying metal poor ([Fe/H] = −1.4) halo found within the inner 70 kpc of M31 (Chapman et al. 2006). Spectroscopic studies of RGB stars along the minor axis of M31 have been prone to inadvertently sampling stream-like substructure (Gilbert et al. 2006; Koch et al. 2008; Chapman et al. 2008), but

they also do find a range of metallicities in the 100–150 kpc regime consistent with the [Fe/H] in these dSph fields.

We have described before in Chapman et al. (2008) the expected probabilities of halo star contamination to fields at these distances. Here, we run a simple Monte Carlo simulation of the expected effect of the contaminant on the observed σ_v. We take two distributions, for the halo (120 km s^{-1} σ_v at 100 kpc projected) and for each dSph as measured here. We then draw randomly from these distributions, asking how often halo stars land in some window indistinguishable from the dSph. We then remeasure the dwarf σ_v whenever star(s) from the halo is present. We find a halo star lands in the And XV window 25 per cent of the time, and in And XVI 9 per cent of the time. In 100 samples with a contaminating halo star(s) lying in the dSph, the velocity dispersion was measured to range 11–12 km s^{-1} (And XV, assumed $\sigma_v = 11$ km s^{-1}) and 8–9 km s^{-1} (And XVI, assumed $\sigma_v = 8$ km s^{-1}). Thus, the affect of halo stars lying in the velocity window is small relative to the errors in estimating σ_v.

We then turn to the orbital properties of these dSphs. And XV lies near the minor axis of M31, at about the same distance and heliocentric velocity as M31 (785 kpc and $v_r \sim -300$ km s^{-1}). As such, its orbit must be close to polar with a large implied tangential velocity component. By contrast, at the large M31-centric distance of And XVI ($\sim$270 kpc), its velocity of ~ -400 km s^{-1} pushes it towards the escape velocity of M31 (assuming the mass modelling of Geehan et al. 2006; see Chapman et al. 2007 Fig. 4 for a depiction of the M31 dwarf galaxies in this context). This is comparable to the orbital properties of other recently discovered dSphs (And XII: Chapman et al. 2007; And XIV: Majewski et al. 2007). In particular, And XII is travelling near the escape velocity of the entire Local Group. Finding so many satellites near the escape velocity of M31 may suggest that the total mass of M31 has been somewhat underestimated to date.

And XVI appears to sit spatially within a preferred distribution of satellites of M31 (Koch et al. 2006; McConnachie & Irwin 2006), falling towards us at $\sim$100 km s^{-1} (with an unknown tangential component). However, And XV sits somewhat outside of this distribution (in both position and likely orbit) and may represent one of the growing number of discovered M31 satellites which hint at a more complicated environment than was apparent with the first generation of discovered satellites.

ACKNOWLEDGMENTS

The data presented herein were obtained at the W.M. Keck Observatory, which is operated as a scientific partnership among the California Institute of Technology, the University of California and the National Aeronautics and Space Administration. The Observatory was made possible by the generous financial support of the W.M. Keck Foundation.

REFERENCES

Bellazzini M., Ferraro F. R., Pancino E., 2001, MNRAS, 327, L15
Belokurov V. et al., 2006, ApJ, 647, L111
Belokurov V. et al., 2007, ApJ, 658, 337
Bullock J. S., Kravstov A. V., Weinberg D. H., 2000, ApJ, 539, 517
Carignan C., Chemin L., Huchtmeier W. K., Lockman F. J., 2006, ApJ, 641, L109
Carretta E., Gratton R., 1997, A&AS 121, 95
Chapman S., Ibata R., Ferguson A. M. N., Lewis G., Irwin M., Tanvir N., 2005, ApJ, 632, L87
Chapman S., Ibata R., Lewis G., Ferguson A. M. N., Irwin M., McConnachie A., Tanvir N., 2006, ApJ, 653, 255
Chapman S. C. et al., 2008, MNRAS, 390, 1437
Chapman S. et al., 2007, ApJ, 662, L79
Evans N., Wilkinson M. I., Guhathakurta P., Grebel E. K., Vogt S., 2000, ApJ, 540, L9
Faber S. M. et al., 2003, Proc. SPIE, 4841, 1657
Fellhauer M. et al., 2007, MNRAS, 375, 1171
Geehan J., Fardal M., Babul A., Guhathakurta P., 2006, MNRAS, 366, 996
Girardi L., Grebel E., Odenkirchen M., Chiosi C., 2004, A&A, 422, 205
Gilbert K. et al., 2006, ApJ, 652, 1188
Gilmore G. et al., 2007, Nucl. Phys. B Proc. Suppl., 173, 15
Gottesman S. T., Hunter J. H., Boonyasait V., 2002, MNRAS, 337, 34
Helmi A. et al., 2006, ApJ, 651, L121
Ibata R., Martin N. F., Irwin M., Chapman S., Ferguson A. M. N., Lewis G. F., McConnachie A. W., 2007, ApJ, 671, 1591
Illingworth G., 1976, ApJ, 204, 73
Irwin M. J., Ferguson A. M. N., Huxor A. P., Tanvir N. R., Ibata R. A., Lewis G. F., 2008, ApJ, 676, L17
Kirby E. N., Simon J. D., Geha M., Guhathakurta P., Frebel A., 2008, ApJ, 685, L43
Klypin A., Kravstov A. V., Velenzuela O., Prada F., 1999, ApJ, 522, 82
Koch A., Grebel E. K., Wyse F. G. W., Kleyna J. T., Wilkinson M. I., Harbeck D. R., Gilmore G. F., Evans N. W., 2006, AJ, 131, 895
Koch A. et al., 2008, ApJ, 689, 958
Kochanek C. S., 1996, ApJ, 457, 228
McConnachie A. W., Irwin M. J., 2006, MNRAS, 365, 1263
McConnachie A., Irwin M., Ferguson A., Ibata R., Lewis G., Tanvir N., 2004, MNRAS, 350, 243
Majewski S. et al., 2007, ApJ, 670, L9
Martin N. F., Ibata R. A., Irwin M. J., Chapman S. C., Lewis G. F., Ferguson A. M. N., Tanvir N., McConnachie A. W., 2006, MNRAS, 371, 1983
Martin N. F., Ibata R. A., Chapman S. C., Irwin M. J., Lewis G. F., 2007, MNRAS, 380, 281
Moore B., Ghigna S., Governato F., Lake G., Quinn T., Stadel J., Tozzi P., 1999, ApJ, 524, L19
Oh K. S., Lin D. N. C., Aarseth S. J., 1995, ApJ, 442, 142
Peñarrubia J., McConnachie A., Babul A., 2006, ApJ, 650, 33
Peñarrubia J., McConnachie A., Navarro J., 2008a, ApJ, 672, 904
Peñarrubia J., Navarro J., McConnachie A., 2008b, ApJ, 673, 226
Piatek S., Pryor C., 1995, AJ, 109, 1071
Richstone D., Tremaine S., 1986, AJ, 92, 72
Shetrone M., Cote P., Sargent W., 2001, ApJ, 548, 592
Schiavon R. P., Barbuy B., Rossi S. C. F., Milone A., 1997, ApJ, 479, 902
Schlegel D., Finkbeiner D., Davis M., 1998, ApJ, 500, 525
Simon J., Geha M., 2007, ApJ, 670, 313
Stoehr F., White S. D. M., Tormen G., Springel V., 2002, MNRAS, 335, L84
Strigari L., Bullock J., Kaplinghat M., Simon J., Geha M., Willman B., Walker M. G., 2008, Nat, 454, 1096
Tollerud E. J., Bullock J. S., Strigari L. E., Willman B., 2008, ApJ, 688, 277
Unavane M., Wyse R., Gilmore G., 1996, MNRAS, 278, 727
Wilkinson M. I., Evans N. W., 1999, MNRAS, 310, 645
Willman B. et al., 2005, AJ, 129, 2692
Zucker D. B. et al., 2004, ApJ, 612, L121
Zucker D. B. et al., 2006a, ApJ, 643, L103
Zucker D. B. et al., 2006b, ApJ, 650, L41

This paper has been typeset from a TEX/LATEX file prepared by the author.